STM JOURNALS

Journal of
Communication Engineering & Systems

ISSN: 2249-8613 (Online)
ISSN: 2321-5151 (Print)
Volume 15, Issue 1, 2025
January–April
DOI (Journal): 10.37591/JoCES

https://journals.stmjournals.com/joces

Review JoCES

Advanced 4-Element UWB-MIMO Antenna Design: Achieving High Isolation and Multi-Band Rejection for Advanced Wireless Applications

Nelly Shafik[1,*], Hazem Hassan Elbanna[2], Sara Kamal Ghazy[3]

Abstract

In this study, we present the design, fabrication, and analysis of a step-by-step Ultra-Wideband (UWB) Multi-Input Multi-Output (MIMO) antenna operating from 3 to 14 GHz. The antenna consists of four elements, each characterized by high isolation and equipped with four band-rejection features. These elements are implemented on a Rogers substrate with ε_r=3. Each antenna element is a modified rectangular patch, incorporating partial ground etching to achieve wider bandwidth. Two sets of U-Shape and H-L shape slots are integrated into the patch to act as band-reject filters. The assigned four-band rejections target frequencies at 5.5 GHz (WLAN), 7.5 GHz (lower X-band), 9.5 GHz (upper X-band), and 12.9 GHz (KU-band). Isolation between antenna elements exceeds 15 dB, effectively reducing mutual coupling. We simulate and calculate MIMO diversity parameters across the entire frequency band which showed acceptable results. Our measured data closely aligns with simulation results, validating the accuracy of this antenna design.

Keywords: Antenna design, element, UWB, MIMO, multi band reject antennas

INTRODUCTION

In recent research on wireless communication systems, Ultra-Wide Band (UWB) technology has emerged as a crucial component due to its high data rate capabilities and cost-effective manufacturing. However, in densely populated mobile coverage areas, multipath fading, caused by reflections and diffractions of electromagnetic waves, poses a significant challenge for UWB technology. To mitigate the effects of multipath fading and enhance performance, Multiple-Input Multiple-Output (MIMO) technology has been integrated with UWB systems [1].

Increasing the number of antennas in a MIMO-UWB system can boost channel capacity without requiring additional frequency bands or power resources. However, this increase in antenna count leads to mutual coupling, which is inversely proportional to the distance between MIMO elements and also affects spatial correlation. For optimal MIMO system performance, mutual coupling should be minimized (less than –15 dB), and the distance between MIMO elements should ideally be between λ/4 and λ/2. Increasing this distance, however, results in a larger MIMO system size [2].

To enhance the performance of wireless communication systems, recent studies have focused on various parameters such as bandwidth, compact size, gain, efficiency, mutual coupling, and diversity in millimeter-wave (mm-Wave) antenna

***Author for Correspondence**
Nelly Shafik
E-mail: nelly_mohammed@yahoo.com

[1]Lecturer, Department of Communication Engineering, Modern Academy for Engineering and Technology, Cairo, Egypt
[2]Student, Department of Electronics Engineering and Communications Technology, Modern Academy for Engineering and Technology, Cairo, Egypt
[3]Student, Department of Electrical Engineering, Faculty of Engineering, Mansoura University, Mansoura, Egypt

Received Date: January 09, 2025
Accepted Date: January 19, 2025
Published Date: February 05, 2025

Citation: Nelly Shafik, Hazem Hassan Elbanna, Sara Kamal Ghazy. Advanced 4-Element UWB-MIMO Antenna Design: Achieving High Isolation and Multi-Band Rejection for Advanced Wireless Applications. Journal of Communication Engineering & Systems. 2025; 15(1): 40–62p.

design. Techniques for optimizing antenna performance include substrate selection and mutual coupling reduction methods. Antenna corrugation, which involves removing metal from the radiator edge, can improve gain, bandwidth efficiency, and front-to-back ratio [3].

One of the main challenges in MIMO technology is the mutual coupling between multiple antenna elements, which can be mitigated using isolation techniques to achieve optimal diversity performance. Various methods have been developed to reduce mutual coupling, including neutralization techniques, simultaneous matching of orthogonal feeding elements, pattern diversity, Defective Ground Structures (DGS), Electromagnetic Band Gap (EBG) structures, substrates, complementary split ring resonators (CSRR), parasitic resonators, and significant polarization techniques [4]. These techniques typically require significant circuit board space. Another approach involves designing MIMO antenna elements with isolating slits, such as F-shaped stubs, T-shaped slots, L-shaped slots, and vertical slots. Testing these designs has shown that mutual coupling can be reduced while maintaining overall gain [5].

In this study, we present a UWB-MIMO microstrip antenna with four band-reject features. Two sets of U-shaped slots and H-L shaped slots are used to create notched bands at 5.5 GHz (WLAN), 7.5 GHz (lower X-band), 9.5 GHz (upper X-band), and 12.9 GHz (KU-band). The H-L slots are integrated into the patch, while the U-shaped slots are placed in the feed line to eliminate port coupling and cover the 3–14 GHz UWB band. The results indicate that the antenna effectively rejects four bands within the operating frequency range. Additionally, the antenna is compact (39×39×1.6 mm³), achieves better than 15 dB port isolation, has a preferred radiation pattern, and maintains a slight gain [6].

BASIC ANTENNA ELEMENT DESIGN

A rectangular UWB patch antenna with a cut ground plane was modeled using CST Microwave Studio. Figure 1(a and b) shows the basic antenna element with a Rogers substrate measuring 19.5×19.5×1.6 mm³, a relative dielectric constant of εr=3, and a loss tangent of 0.001. Figure 2 presents the reflection coefficient (S11 in dB) across the 2–14 GHz band for the basic element before modification, yielding initially adequate results [7]. The initial dimensions of the element are listed in Table 1.

It is well-known that using a partial ground plane in microstrip antennas can significantly enhance bandwidth by reducing surface wave losses, thereby improving overall efficiency and bandwidth. This is achieved by enhancing impedance matching and reducing return loss [8]. Adding a beveled tip to the basic element further extends the impedance bandwidth (Figure 3), particularly in the higher frequency range, as illustrated in Figure 4. The results show that S11 is less than –10 dB across the frequency band from approximately 3.7 to 14 GHz.

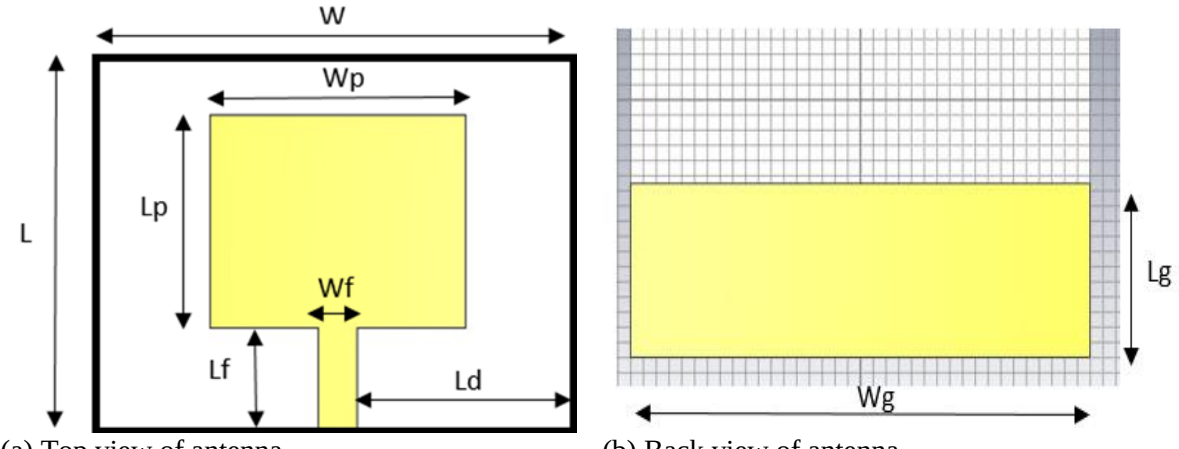

(a) Top view of antenna. (b) Back view of antenna.

Figure 1. Single basic element of UWB antenna, geometrical characteristics.

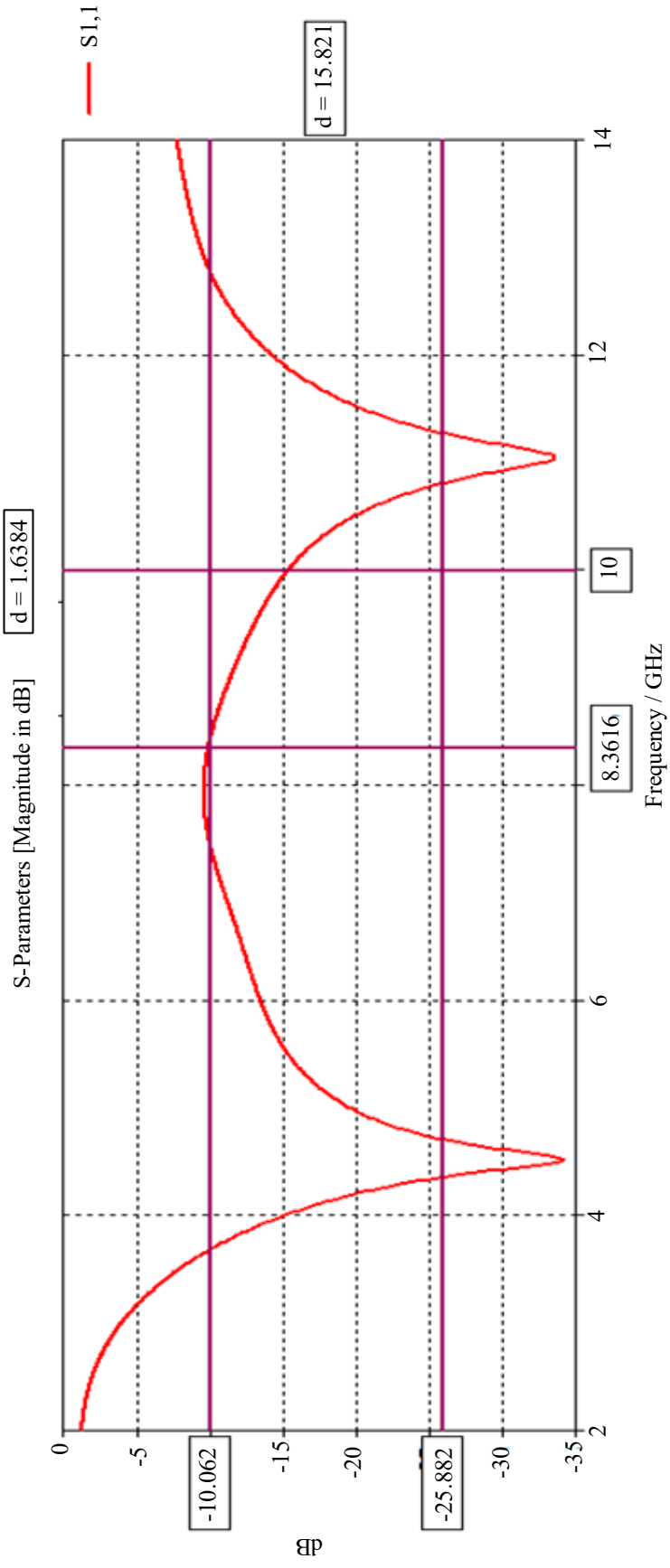

Figure 2. S_{11} of basic single element Antenna.

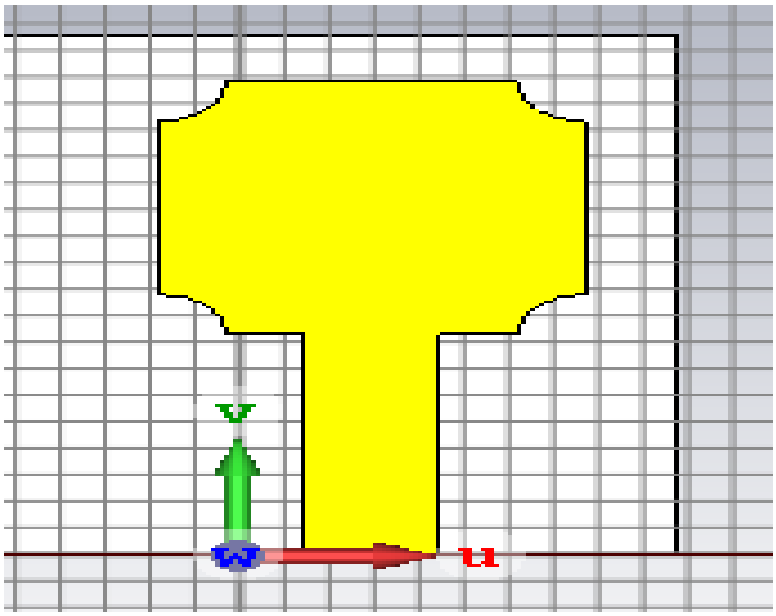

Figure 3. Single element with beveled tip.

Table 1. Dimensions of the proposed basic antenna element.

Parameter	W	L	H	Wp	Lp	Lf	Wf	Ld	Lg	Wg
Value (mm)	19.5	19.5	1.6	9.3	9.5	8.3	3	5.3	5.8	18.5

U Shape Slot

A U-shaped slot is introduced in the feeding line, with its size primarily determining the first notch (6.8–8 GHz), as shown in Figure 5. The reflection coefficient (S11) remains below –10 dB across the operating band, except for the first notch band centered at 7.5 GHz, as illustrated in Figure 6.

H-L Shape Slot

An H-L shaped slot is incorporated into the patch, creating three notches at center frequencies of 5.5, 9.5, and 12.9 GHz. Figure 7 illustrates the geometrical structure of the H-L shape within the patch, while Figure 8 shows the reflection coefficient (S11) across the entire operating band [9]. The S11 remains below –10 dB, except at the specified notch bands.

ANTENNA ELEMENT DESIGN AND OPTIMIZATION

CST software and MATLAB were used to design and simulate the proposed antenna. Figure 9(a and b) and Table 2 illustrate the geometry and dimensions of the antenna [10]. The substrate used is Rogers with a relative permittivity of 3, a thickness of 1.6 mm, and a surface area of 19.5×19.5 mm². The 50 Ω microstrip feed line has dimensions of 3 mm in width and 8.3 mm in length [11].

In this design, four notch bands were created to avoid interference with existing communication networks within the 2–14 GHz frequency range. These notch bands have central frequencies of 5.5, 7.5, 9.5, and 12.9 GHz. The notches are achieved using a U-shaped slot in the feed line and an H-L shaped slot in the radiation patch, as shown in Figure 9. The specific bands are the 5.5 GHz WLAN band, the lower X-band (6.9–7.7 GHz), the upper X-band (9.3–9.7 GHz), and the Ku-band (12.2–13.1 GHz) [12].

The first notch (5.1–5.8 GHz), the second notch (12.2–13.1 GHz), and the fourth notch (9.3–9.7 GHz) are primarily determined by the dimensions of the H-L slot (Ls1, Ls3, Ls4, Ls5, and S1). The third notch (6.7–7.7 GHz) is governed by the dimensions of the U-shaped slot (Y1 and S2). Table 2 provides the optimized dimensions of the proposed antenna element [13].

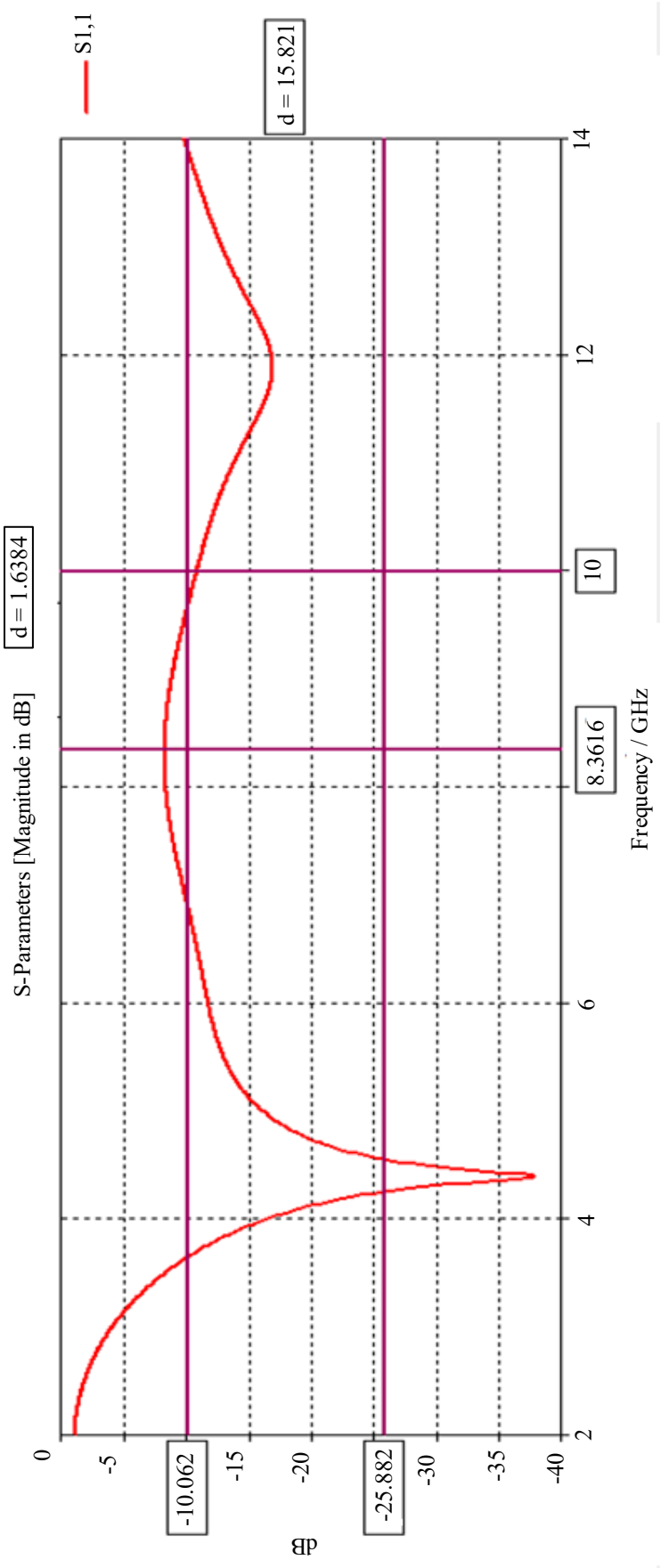

Figure 4. S_{11} parameter of the basic element with beveled corners.

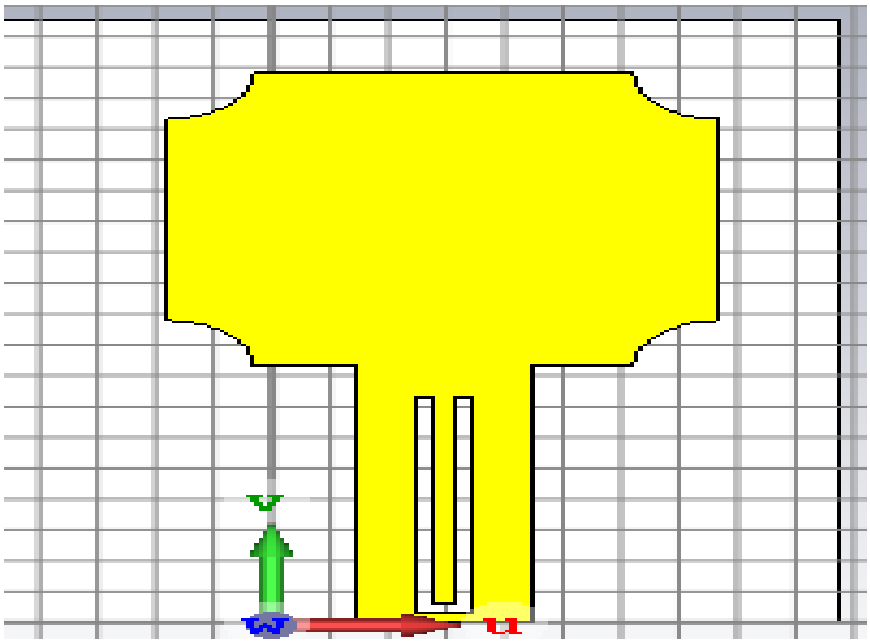

Figure 5. Geometry of the UWB antenna with U shape slot.

Table 2. Dimensions of the proposed UWB antenna.

Parameter	Value (mm)	Parameter	Value (mm)
W	*19.5*	*Lg*	*5.8*
L	*19.5*	*Wg*	*18.5*
h	*1.6*	*Y1*	*7*
Wf	*3*	*Ls3*	*2.3*
Lf	*8.3*	*Ls2*	*3.7*
Ld	*5.3*	*Ls1*	*7.4*
R	*1.5*	*Ls5*	*2.75*
Ls4	*6*	*Y2*	*1*
S1=S2	*0.3*	*Lp*	*9.5*

SIMULATION RESULTS OF THE ANTENNA-ELEMENT

Figure 10(a and b) illustrate the reflection coefficient and VSWR, respectively, for the proposed element design [14]. The simulation results show very satisfactory performance, with S11 remaining below –10 dB across the entire operating band, except at the four designated notch frequencies. The inclusion of different slots and a partial ground plane alters the current distribution on the antenna, supporting multiple resonant frequencies and enabling various band rejections. The simulated surface current distribution at different notch bands is shown in Figure 11(a–d). Consequently, there is either no radiation or very minimal radiation at these frequencies, which increases the antenna's return loss [15].

DESIGN AND RESULTS OF UWB-MIMO ANTENNA

UWB-MIMO Antenna Structure

This design consists of four antenna elements orthogonal to each other as shown in Figure 12 to reduce mutual coupling between them [16]. By this configuration, the MIMO antenna had a port isolation less than −15 dB without any decoupling elements. Main antenna parameters are mentioned in Table 2; the volume is reduced to 39×39×1.6 mm^3.

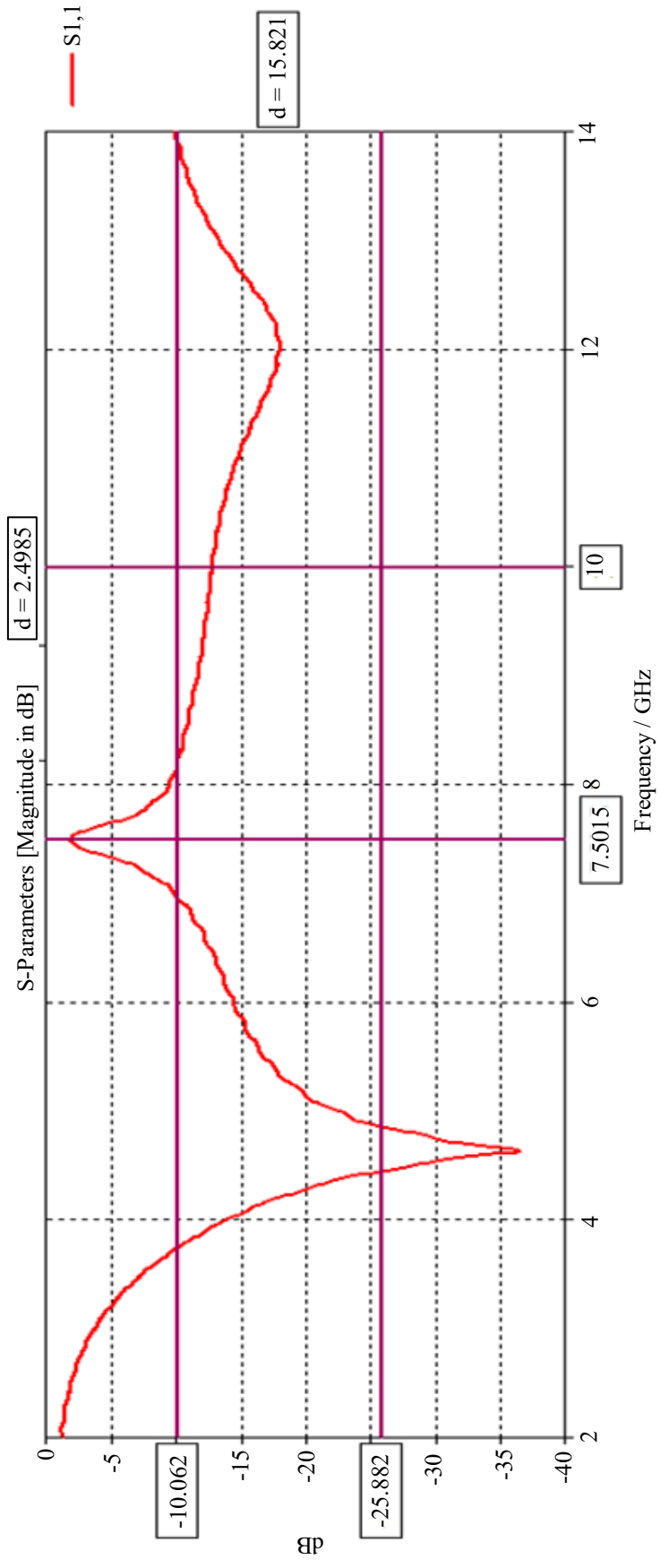

Figure 6. S_{11} of the single antenna design with notch center frequency at 7.5 GHz.

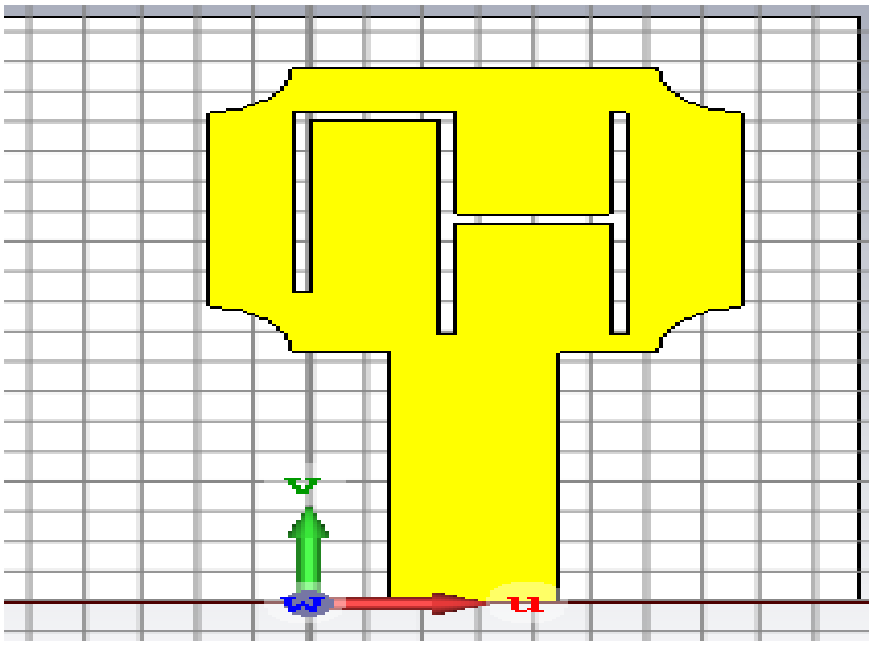

Figure 7. Geometry of the UWB antenna with H-L slot shape.

Simulation Results (S11 and Mutual Coupling)

CST software, in conjunction with MATLAB, was used to simulate the proposed UWB-MIMO antenna, excluding the four rejected bands. The reflection coefficients S11, S22, S33, and S44 are shown in Figure 13, remaining below –10 dB from 3 to 14 GHz, except at the four notch bands [17].

Figure 14 illustrates the mutual coupling between elements 1, 2, 3, and 4 when one of the four ports is excited and the other three ports are terminated with 50 Ω matched loads. Due to symmetry, only the S parameters S12, S13, S14, S23, S24, and S34 are displayed. The results indicate that the isolation between ports is acceptable, with the transmission coefficient remaining below –15 dB across the entire band [18].

Radiation Patterns

The far-field radiation patterns of the suggested UWB-MIMO antenna are shown in Figure 15. It is shown that the radiation is approximately uniform in different planes. The x-z plane and the y-z plane at four distinct frequencies of 5.5, 7.5, 9.5 and 12.9 GHz are displayed [19]. It is significant to remember that the MIMO antenna is y-polarized and printed on the x-y plane, x-z plan is the H-plane and the y-z plane is the E-plane.

As shown in Figure 15, the radiation pattern in the H-plane is essentially omnidirectional, whereas the radiation pattern in the E-plane is more resembling a dumb-bell at almost all operating frequencies, including the notch frequencies [20].

FABRICATION AND MEASUREMENTS

The UWB-MIMO antenna depicted in Figure 16(a and b) is fabricated on a ROGER PCB. Measurements are conducted using a Rohde and Schwarz ZVB-20 vector network analyzer. The measurement and simulation results are closely aligned and within acceptable ranges [21].

Figure 17(a) illustrates the variation between the S11 measurement and simulation of the MIMO antenna, while Figure 17(b) highlights the differences between the simulation and measurement of the mutual coupling among the four elements.

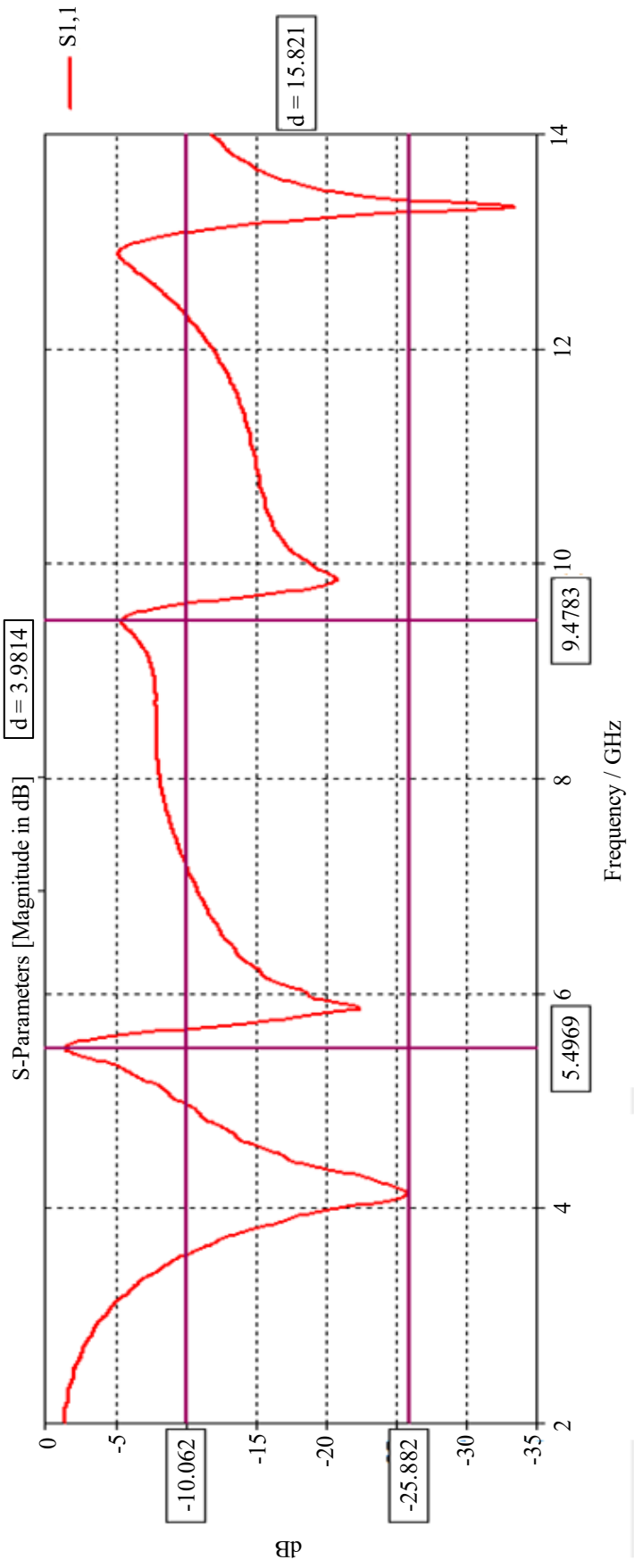

Figure 8. S_{11} of the single antenna design with center frequency 5.5, 9.5, 12.9 GHz notched bands.

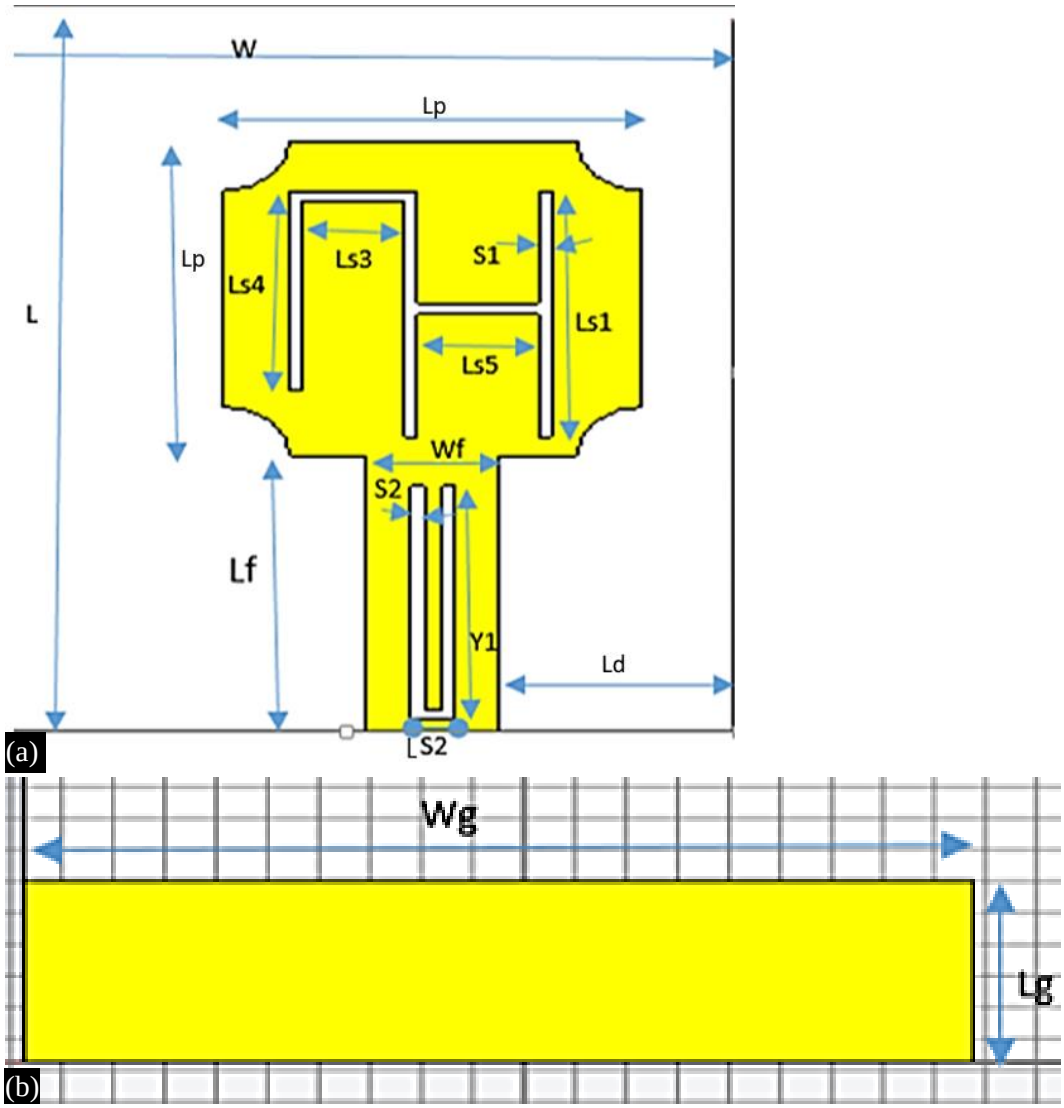

Figure 9. Geometry of the UWB antenna with four notched-bands. (a) Top view of proposed antenna, (b) Back view of proposed antenna.

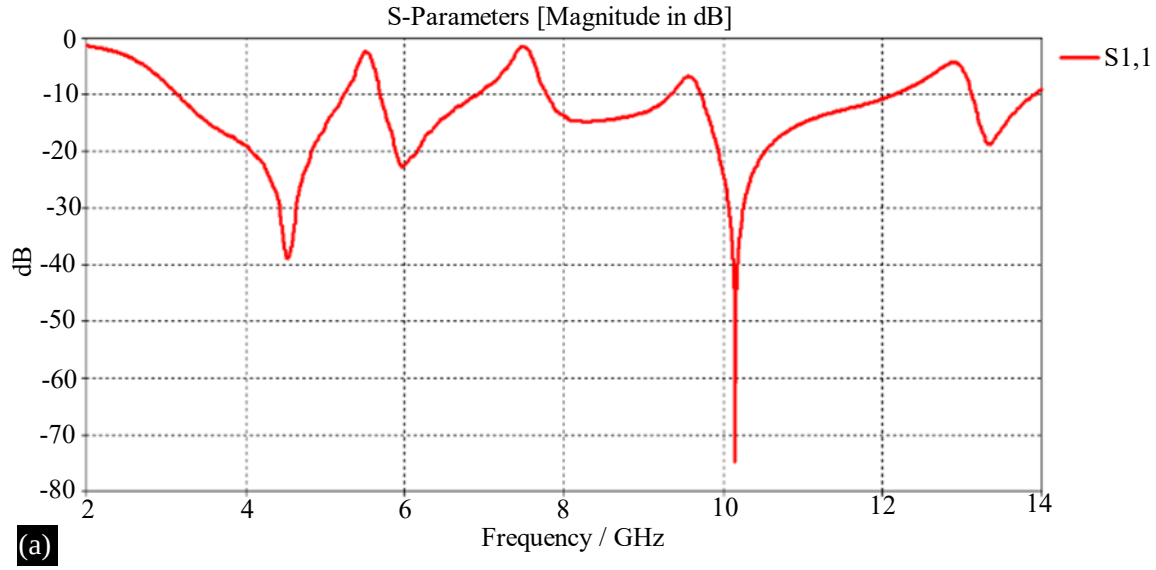

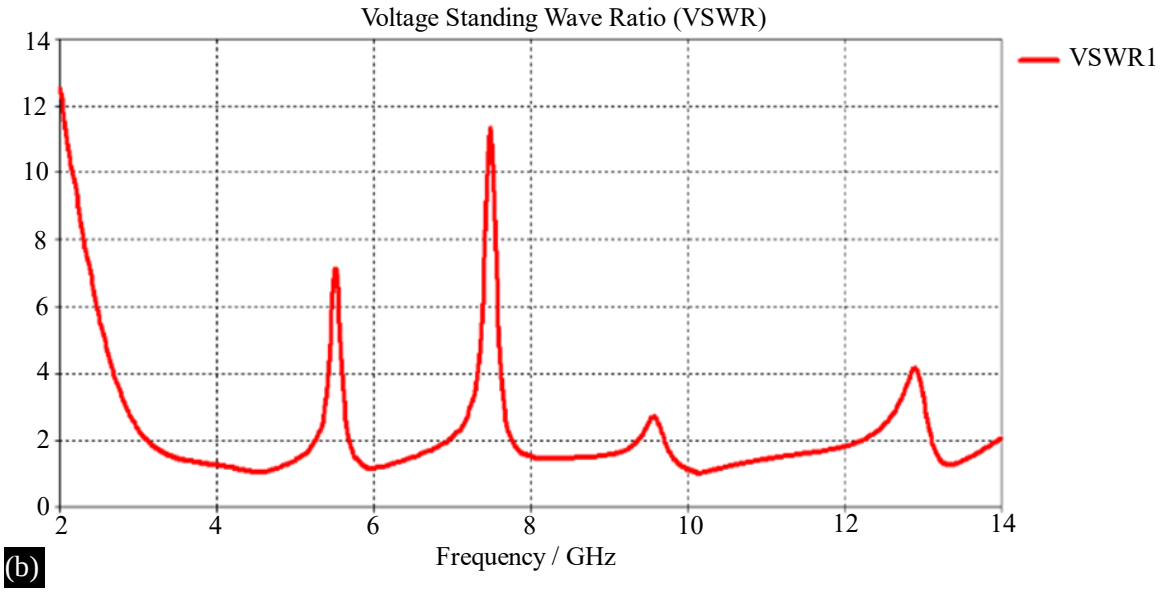

Figure 10. simulation results of a single element (a) S_{11} and (b) VSWR.

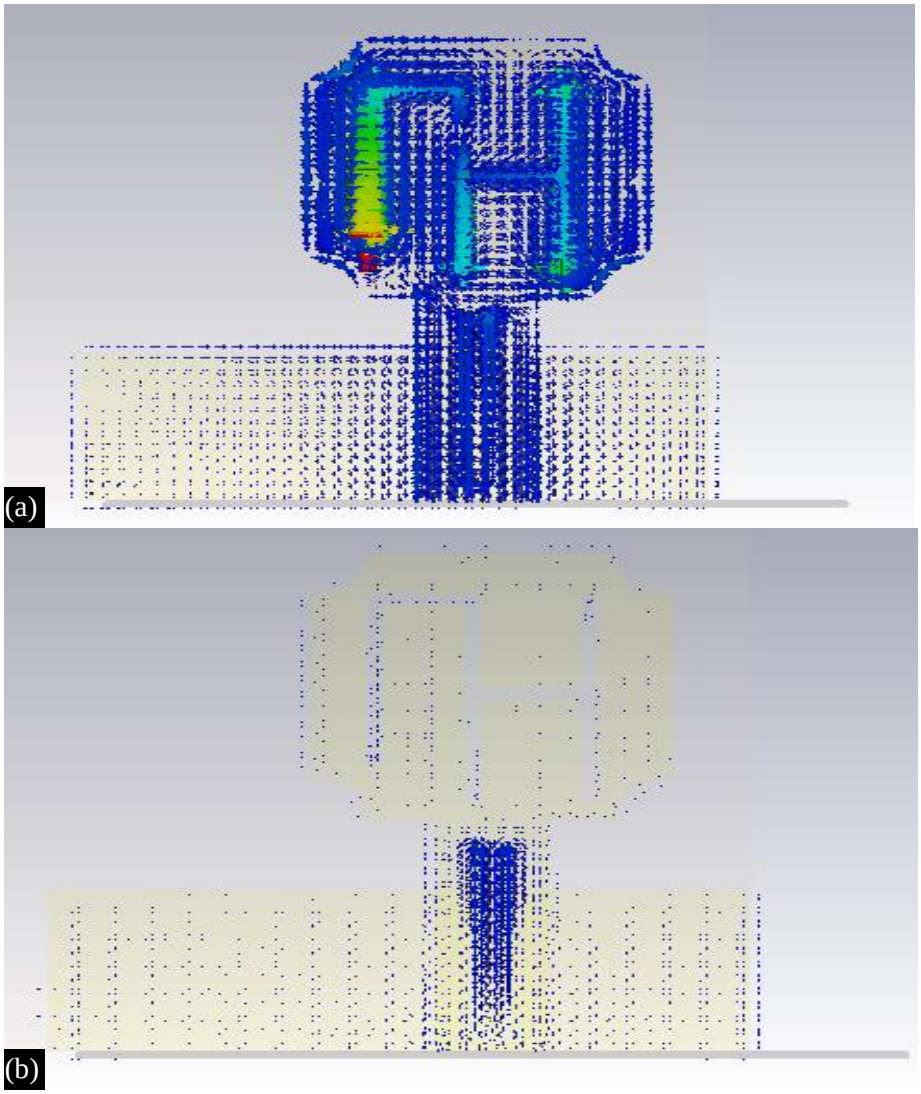

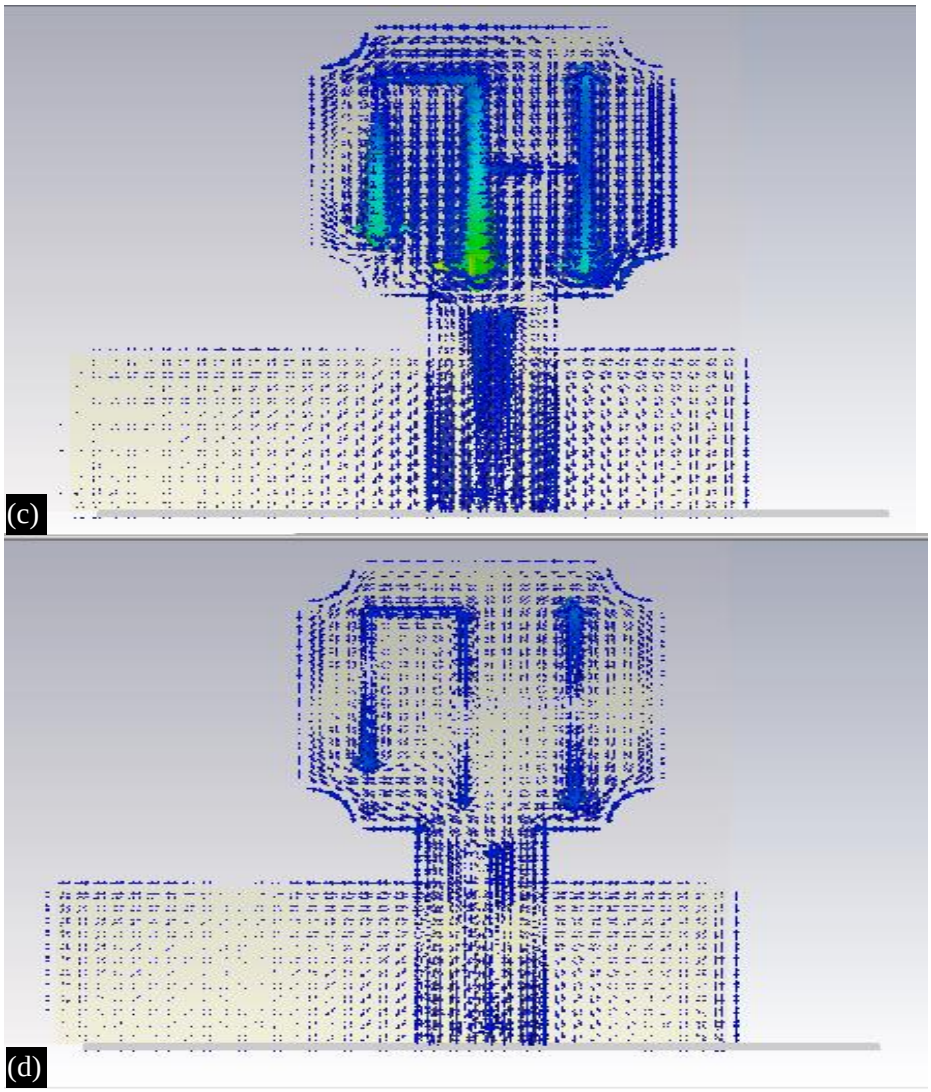

Figure 11. (a) Surface current distribution at 5.5 GHz. (b) Surface current distribution at 7.5 GHz, (c) Surface current distribution at 9.5 GHz, (d) Surface current distribution at 12.9 GHz.

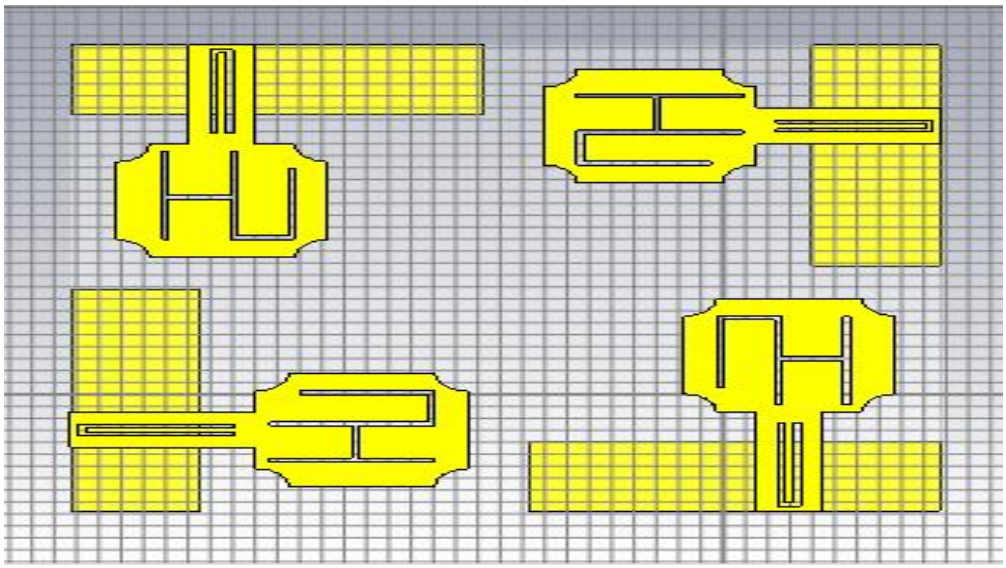

Figure 12. The proposed UWB-MIMO antenna Layout.

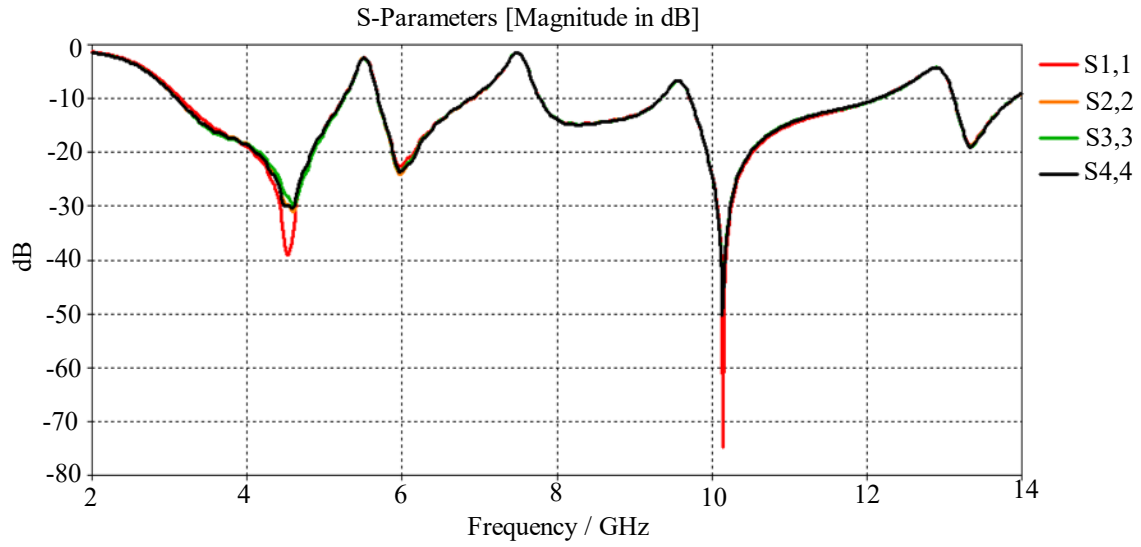

Figure 13. S_{11}, S_{22}, S_{33} and S_{44} of the MIMO antenna with four band-reject.

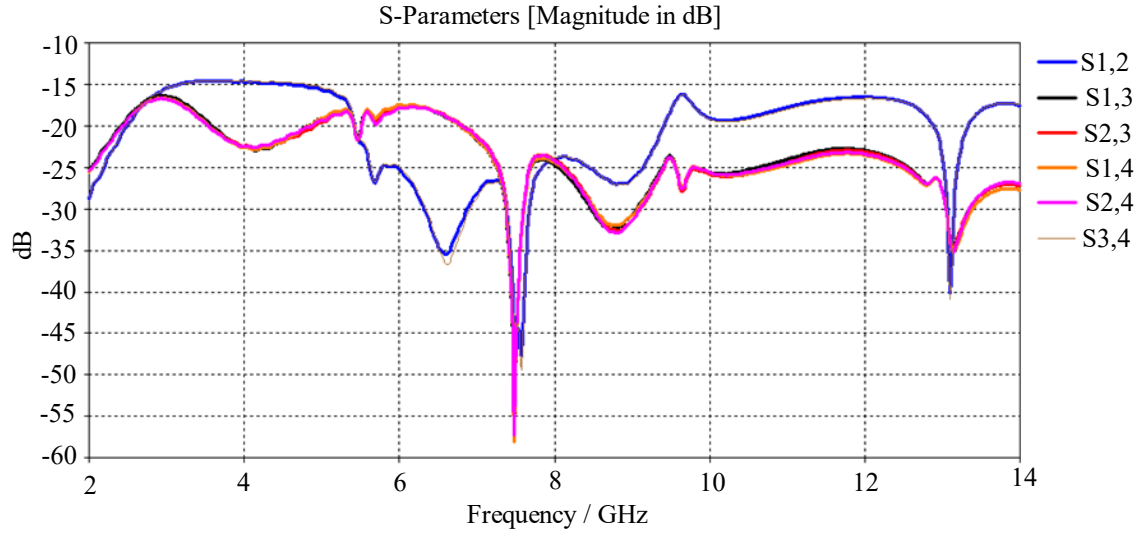

Figure 14. S-parameter of MIMO antenna (S_{12}, S_{13}, S_{14}, S_{23}, S_{24} and S_{34}).

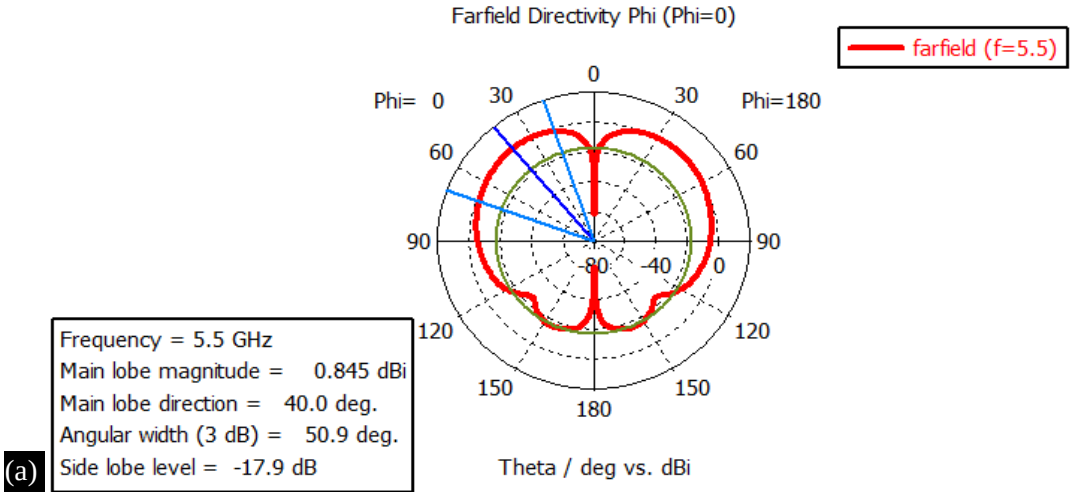

(a)

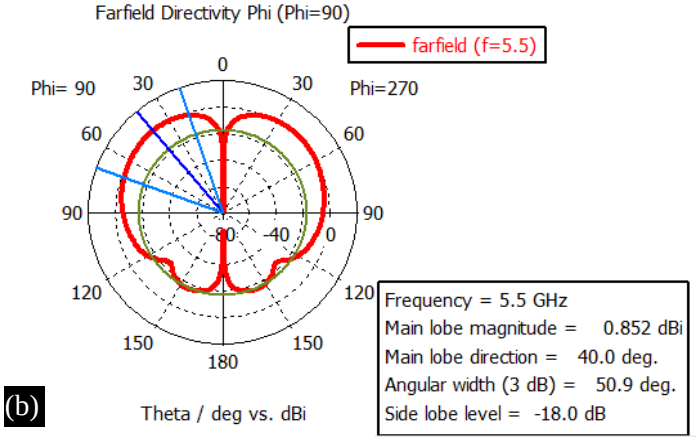

(b)

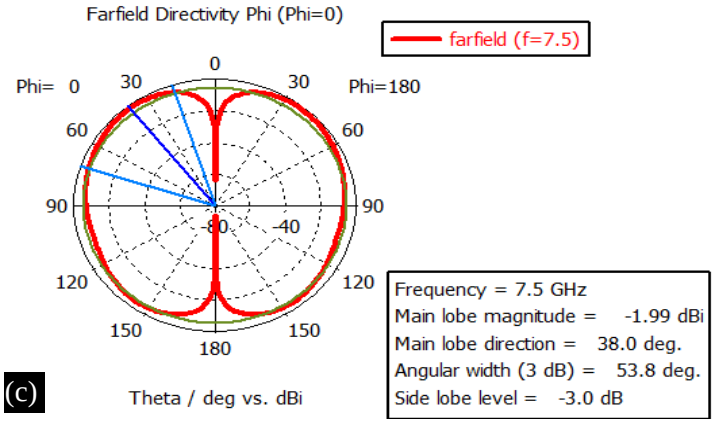

(c)

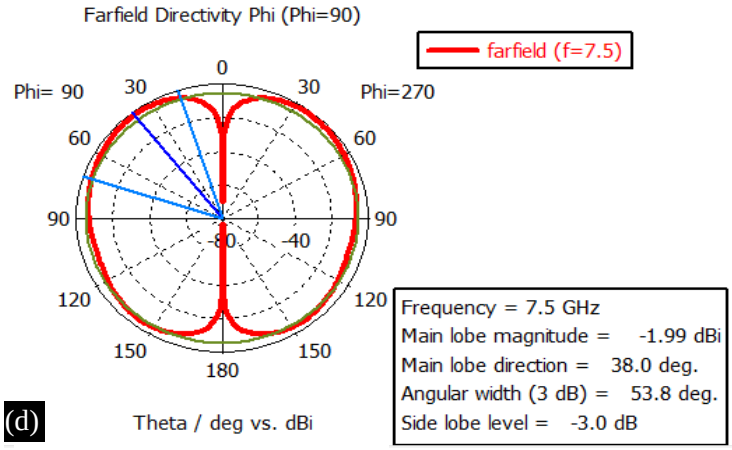

(d)

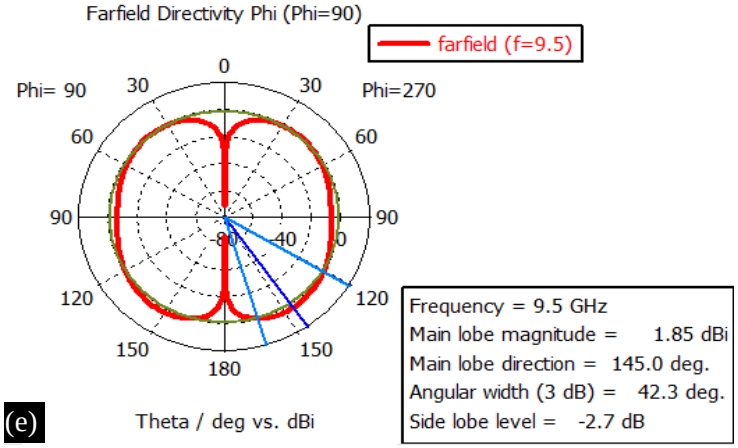

(e)

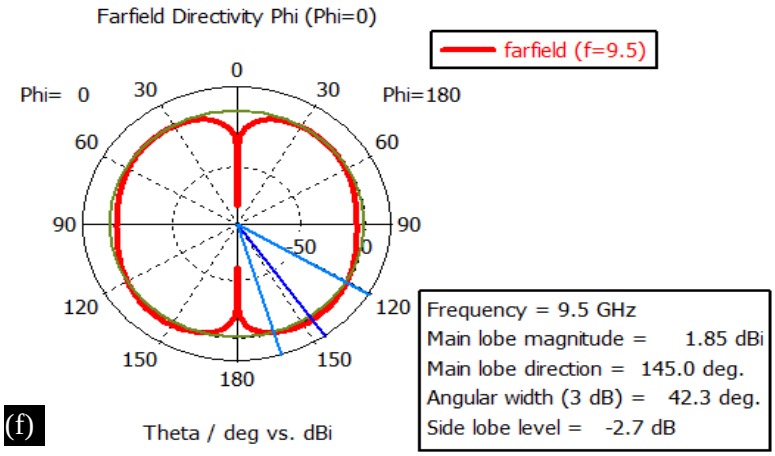

(f)

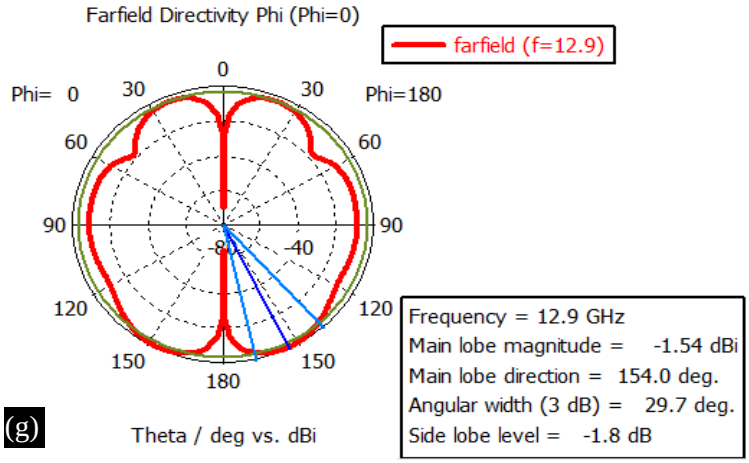

(g)

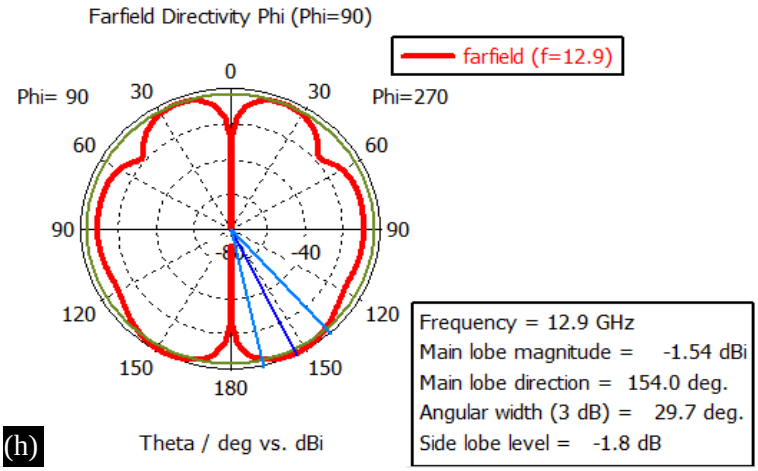

(h)

Figure 15. (a–h) Simulations of the UWB-MIMO design's radiation patterns in the H-plane and E-plane at various frequencies: 5.5, 7.5, 9.5, and 12.9 GHz.

DIVERSITY CHARACTERISTICS

Envelope Correlation Coefficient (ECC)

Diversity in a MIMO antenna system requires the radiation patterns of the antenna components to be uncorrelated [22]. The Envelope Correlation Coefficient (ECC) measures the correlation between signals received or transmitted by different antenna elements. A lower ECC signifies better diversity performance. It can be derived from radiation patterns or S-parameters and serves as a metric for evaluating the correlation between radiation patterns. The ECC can be calculated using Eq. (1) [23].

$$\mathrm{ECC} = \rho e^{(i,j,N)} = \frac{\left|\sum_{n=1}^{N} s_{i,n}^{*} s_{n,j}\right|^{2}}{\prod_{k=(i,j)}\left[1-\sum_{n=1}^{N} s_{i,n}^{*} s_{n,k}\right]} \quad (1)$$

For instance, for (i=1), (j=2), and (N=4), $\rho e^{(i,j,N)}$ represents the Envelope Correlation Coefficient (ECC) between antennas (i) and (j) in the (N)-element MIMO antenna system. The ECC for the proposed four-element MIMO system is computed across the entire operating frequency range (3–14 GHz) using the simulated S-parameters, as shown in Figure 18. The ECC values are calculated over the 3–14 GHz band, and it is known that the ECC should be below 0.5 for strong diversity performance [24]. The observed ECC is significantly less than 0.025 across the entire frequency spectrum, indicating a very low correlation with the proposed UWB-MIMO antenna. This results in excellent diversity performance between the antenna elements, with ECC values consistently below 0.025.

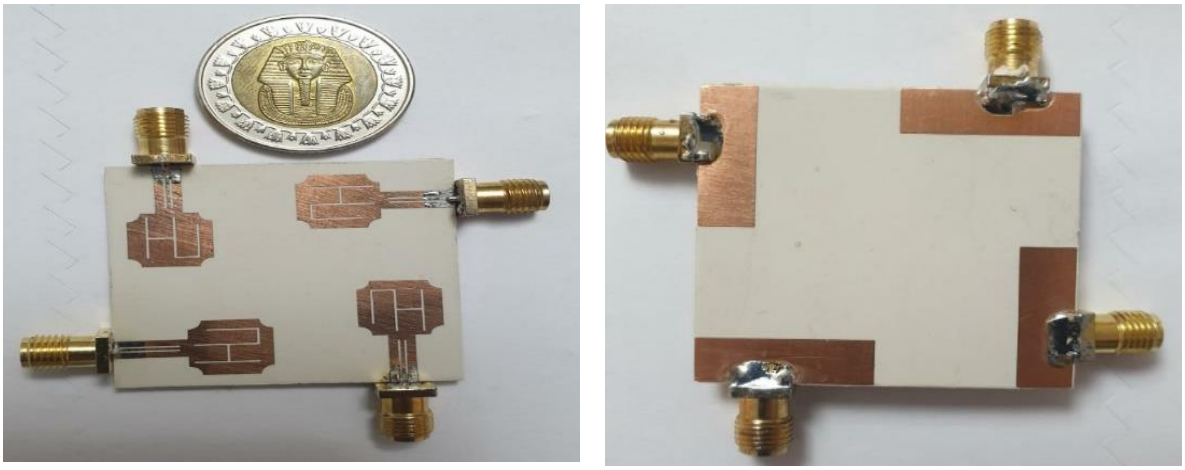

(a) Top view layout. (b) Back view layout.

Figure 16. Fabrication of the UWB antenna with four notched-bands.

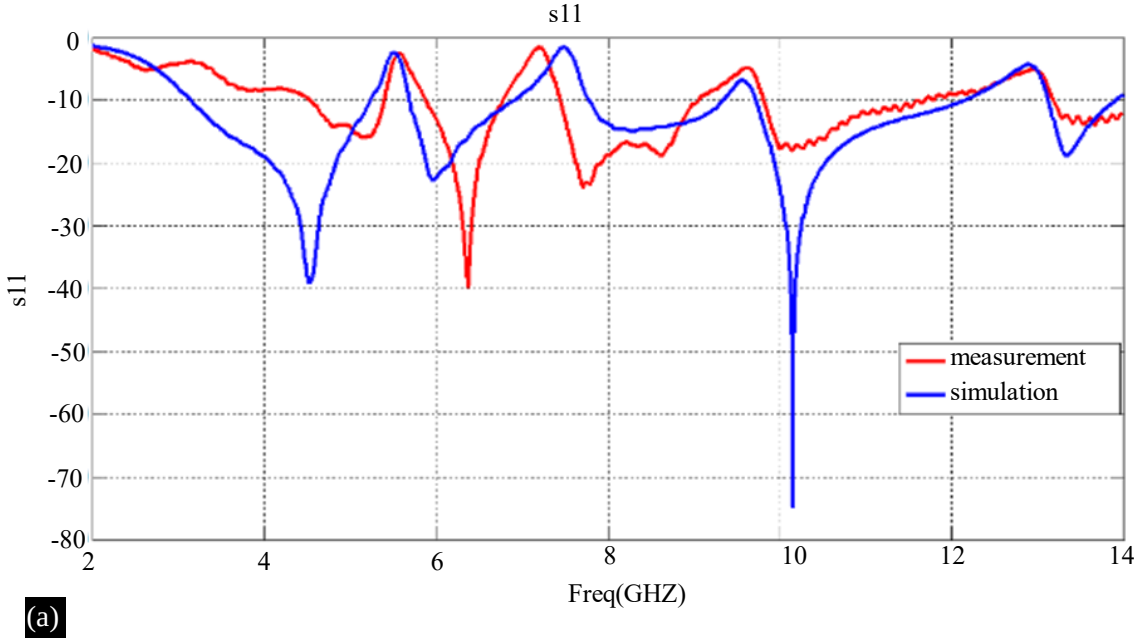

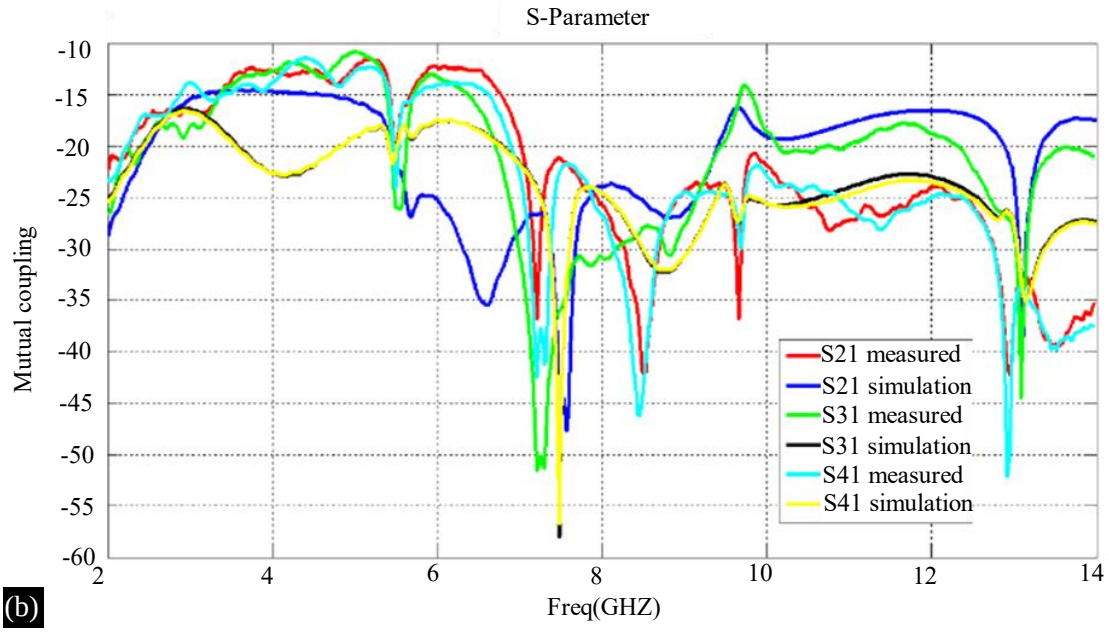

Figure 17. Simulation and measurements of S-parameter of MIMO antenna. (a) S11 measured and simulated, (b) S21, S31, S41 measured and simulated.

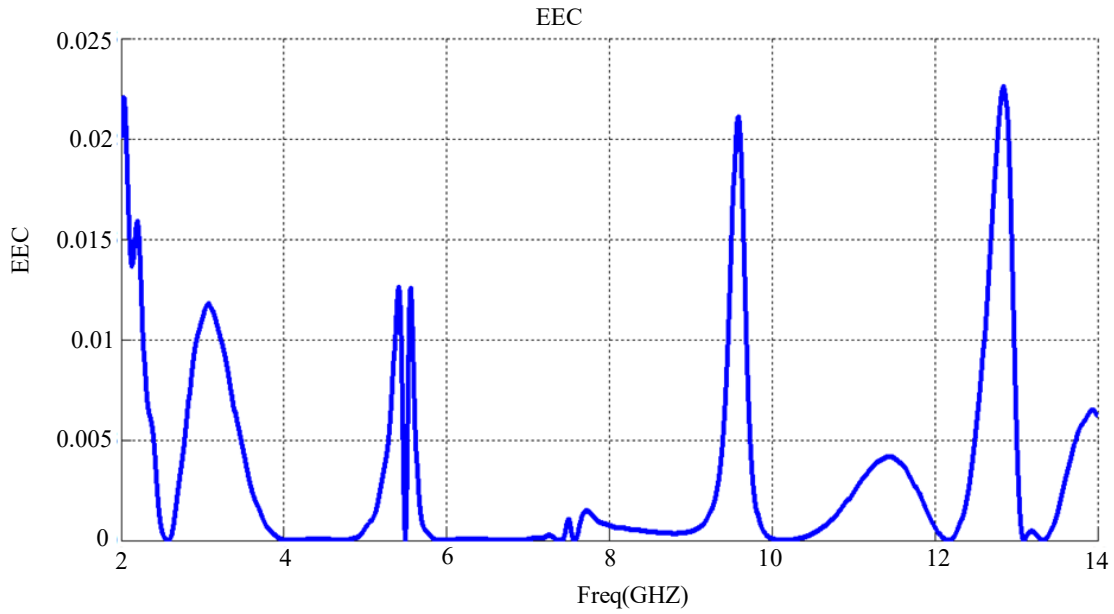

Figure 18. Performance of the suggested UWB-MIMO antenna under simulated MIMO diversity: ECC.

Diversity Gain (DG)

Diversity gain refers to the enhancement in signal quality and reliability achieved by employing multiple antennas at both the transmitter and receiver ends of a communication link. By increasing the number of antennas, MIMO techniques improve channel capacity without the need for additional power or spectrum resources. Essentially, diversity gain mitigates the adverse effects of fading and interference in wireless channels. The following equation can be used to express diversity gain (DG) [25]:

$$DG = 10\sqrt{1 - ECC^2} \tag{2}$$

Figure 19 shows the diversity gain (DG) values across different frequencies. It is noteworthy that the DG of the proposed UWB MIMO antenna is consistently greater than 9.9 dB and exceeds 10 dB throughout the operating frequency range of 2–14 GHz. This indicates a high diversity gain for the proposed UWB MIMO antenna.

Channel Capacity Loss (CCL)

Channel capacity loss (CCL) refers to the decrease in the maximum rate at which information can be reliably transmitted over a communication channel.

An acceptable CCL value is 0.4 bps/Hz. The S-parameter can be used to calculate the CCL of the 4-element UWB-MIMO system using the following equation [26]:

$$CCL = -\log_2 \det\left(\psi^R\right) \tag{3}$$

Where ψ^R is the 4-element MIMO antenna correlation matrix for receiving antennas (R=4), can be expressed as:

$$\psi^R = \begin{vmatrix} p_{11} & p_{12} & p_{13} & p_{14} \\ p_{21} & p_{22} & p_{23} & p_{24} \\ p_{31} & p_{32} & p_{33} & p_{34} \\ p_{41} & p_{42} & p_{43} & p_{44} \end{vmatrix} \tag{4}$$

Where $p_{ii} = 1 - \left|\sum_{n=1}^{N=4} s_{i,n}^* s_{n,i}\right|$ and $p_{ij} = -\left|\sum_{n=1}^{N=4} s_{i,n}^* s_{n,j}\right|$ i, j=1, 2, 3 or 4

After computing the CCL using Eq. (3), the results are displayed in Figure 20. It can be observed that the CCL is less than 0.3 bps/Hz across the entire band, except for the four notch bands where it exceeds the acceptable value of 0.4 bps/Hz.

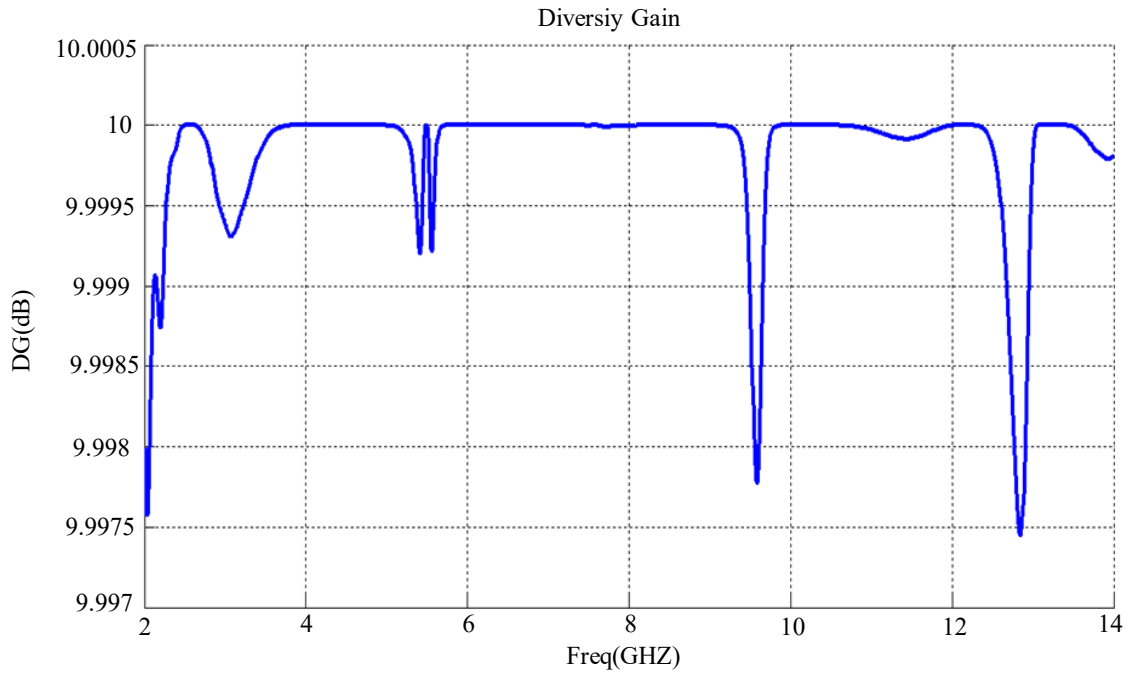

Figure 19. Performance of the suggested UWB-MIMO antenna under simulated MIMO diversity: DG.

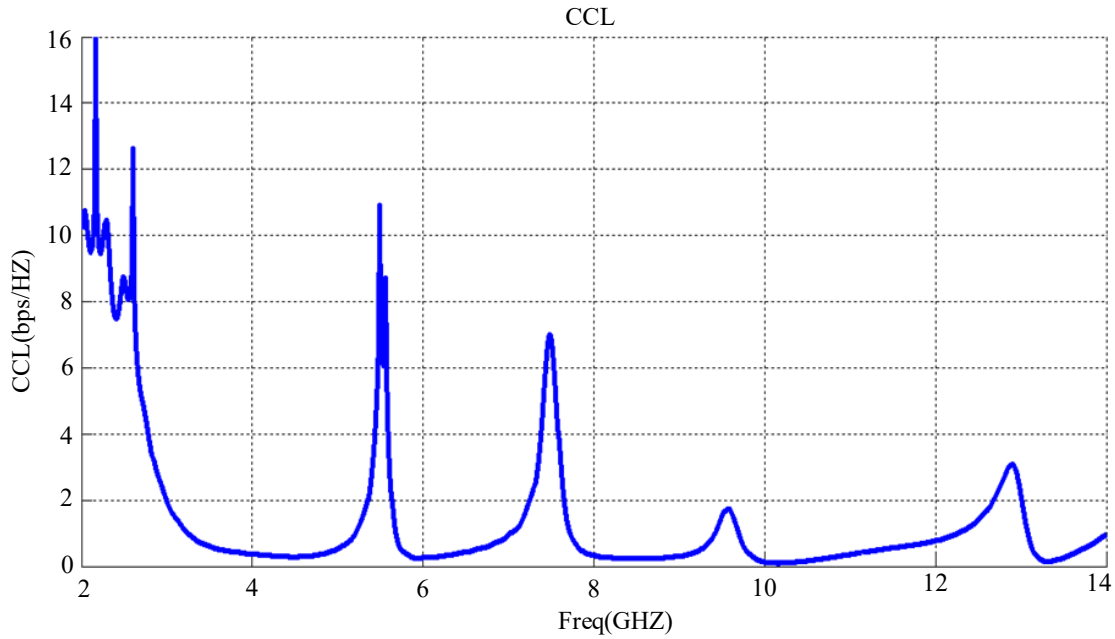

Figure 20. Performance of the suggested UWB-MIMO antenna; the calculated CCL.

Multiplexing efficiency (ME)

Multiplexing efficiency quantifies how effectively a MIMO system can transmit or receive data compared to an ideal reference system. It measures the system's ability to utilize multiple antennas to transmit independent data streams. This efficiency can be influenced by various factors, including channel conditions, antenna design, and user effects. The design and placement of antennas significantly impact efficiency. Well-designed antennas with good isolation and low mutual coupling can maintain high efficiency over a wide range of conditions. In practical terms, the dynamic range of multiplexing efficiency in MIMO systems can vary from nearly 0% in very poor conditions to close to 100% in optimal conditions. In this design, the multiplexing efficiency (ME) in the four frequency bands (5.5, 7.5, 9.5, and 12.5 GHz) is greater than –3 dB, indicating high efficiency for the UWB-MIMO antenna (2–14 GHz). It only decreases to –3 dB at the lower narrow band, as shown in Figure 21.

The multiplexing efficiency (η_{mux}) is calculated by using Eq. (5) [27]:

$$\eta_{mux} = \sqrt{\eta_i \eta_j \left(1 - |pe|^2\right)} \tag{5}$$

Where η_i, η_j is the total efficiency of the ith, jth antenna port, which extracted from CST program.

Total active reflection coefficient (TARC)

TARC (Total Active Reflection Coefficient) relates the total incident power to the total outgoing power in an N-port microwave component, quantifying the amount of incident power that is reflected back. Figure 22 shows the TARC of the designed antenna, calculated using Eq. (6) [28, 29]. The calculated TARC values are within acceptable ranges across the entire band, justifying the four-band rejection as well.

$$TARC = N^{-0.5} \sqrt{\sum_{i=1}^{N} \left| \sum_{k=1}^{N} s_{ik} e^{j\vartheta(k-1)} \right|^2} \tag{6}$$

For N=4, $\boldsymbol{\theta}$=0:180, i, k=1:4

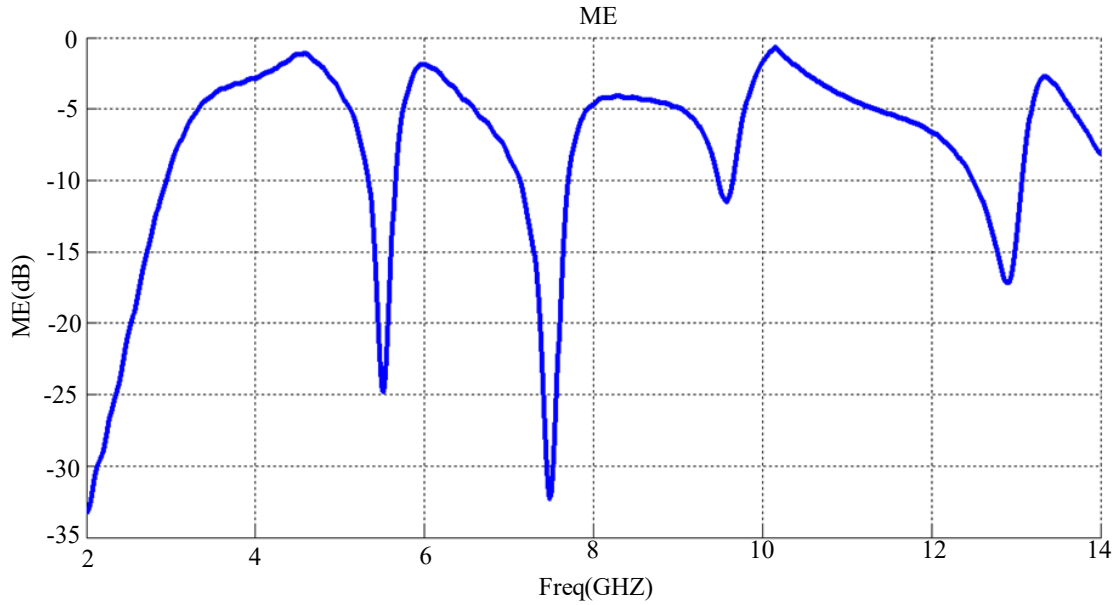

Figure 21. Performance of the suggested UWB-MIMO antenna diversity calculated: ME.

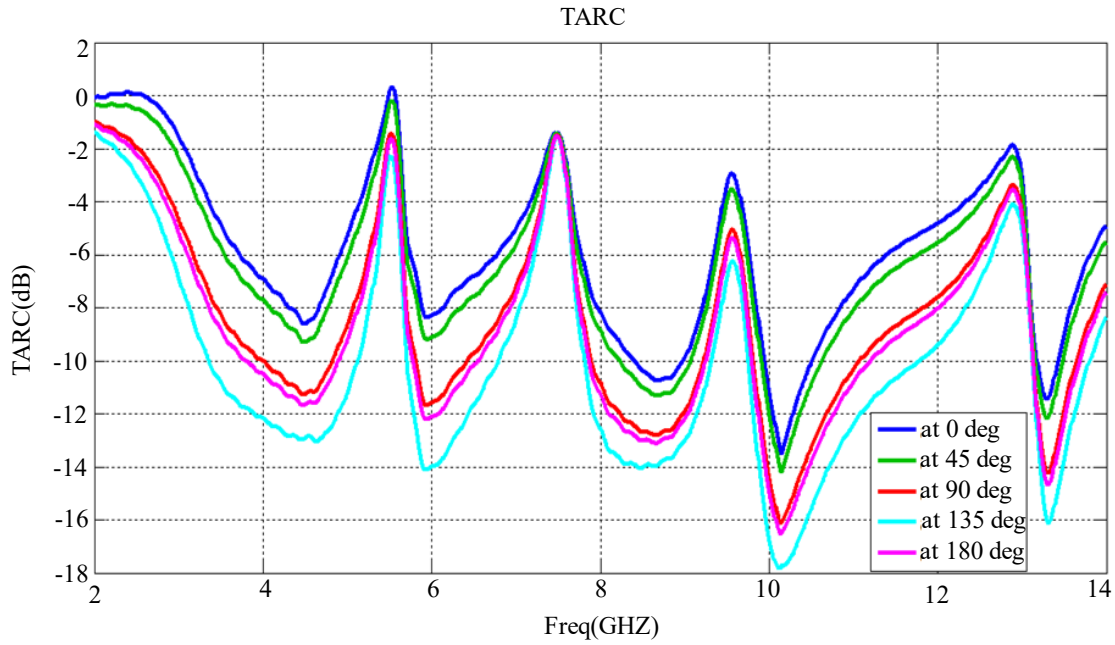

Figure 22. Performance of the suggested UWB-MIMO antenna diversity calculated: TARC.

Mean effective gain (MEG)

The Mean Effective Gain (MEG) is a crucial diversity parameter for MIMO antennas, defined as the ratio of power received by the MIMO antenna to the power received by an isotropic antenna. This performance metric takes into account practical conditions in specific environments. The generalized MEG expression for various propagation models is given by Eq. (7) [24, 30]. It is evident that the maximum MEG value for any port is 0.5, and ideally, the ratio between the MEG of any port and another port should be close to unity.

$\left|\frac{MEG_i}{MEG_j}\right| \approx 1$, and with acceptable value to be ≤3 dB.

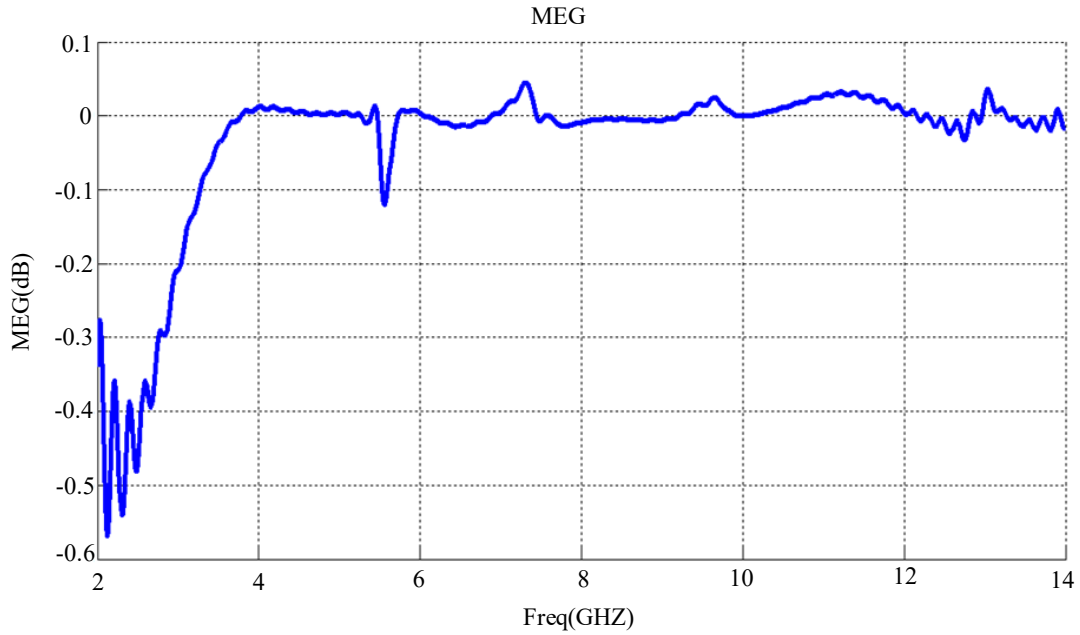

Figure 23. Mean Effective Gain ratio of port 1 and 2 in MIMO antenna.

$$MEG_j = 0.5\left(1 - \sum_{i}^{n}\left|S_{ij}\right|^2\right) \quad (7)$$

Where: i, j= port number, n= number of antenna elements.

Figure 23 shows the ratio between MEG (i) port and MEG (j) port, and it is clear that it is near to unity, 0 dB.

CONCLUSION

This study introduces advanced 4-element UWB-MIMO antenna design that achieves ultra-wideband (UWB) operation, high isolation, and four band rejections for the 5.5 GHz WLAN, low X-band (6.9–7.7 GHz), upper X-band (9.3–9.7 GHz), and KU band (12.2–13.1 GHz). The UWB-MIMO antenna was designed and optimized using CST software. The proposed design was developed and tested, with measurement results closely matching simulation outcomes, demonstrating the effectiveness of the suggested UWB-MIMO antenna. Various parameters, including reflection coefficients, radiation patterns, and coupling, were analyzed to evaluate the design's performance. Across the bandwidth of interest (3–14 GHz), MIMO metrics such as ECC, DG, CCL, ME, MEG, and TARC were calculated. The simulation and measurement results confirm that the proposed design successfully encompasses the entire UWB spectrum while achieving the intended band rejections. The design also achieves high isolation (>20 dB) among antenna components without using disassembly structures. Additionally, it exhibits superior performance with CCL (<0.3 bits/s/Hz), ME (>–3 dB), TARC (<–10), ECC (<0.0015), and DG (>9.8 dB).

REFERENCES

1. Katalinic A, Nagy R, Zentner R. Benefits of MIMO systems in practice: increased capacity, reliability and spectrum efficiency. In IEEE Proceedings ELMAR 2006. 2006 Jun 7; 263–266.
2. Molisch AF, Win MZ. MIMO systems with antenna selection. IEEE Microw Mag. 2004 Mar; 5(1): 46–56.
3. Matta L, Sharma B, Sharma M. A review on bandwidth enhancement techniques and band-notched characteristics of MIMO-ultra wide band antennas. Wirel Netw. 2024 Apr; 30(3): 1339–82.

4. Paulraj AJ, Gore DA, Nabar RU, Bolcskei H. An overview of MIMO communications-a key to gigabit wireless. Proc IEEE. 2004 Feb; 92(2): 198–218.
5. Nadeem I, Choi DY. Study on mutual coupling reduction technique for MIMO antennas. IEEE Access. 2018 Dec 7; 7: 563–86.
6. Honari MM, Ghaffarian MS, Mousavi P, Sarabandi K. A Wideband High-Gain Planar Corrugated Antenna. In 2020 IEEE International Symposium on Antennas and Propagation and North American Radio Science Meeting. 2020 Jul 5; 7–8.
7. Dey S, Dey S, Koul SK. Isolation improvement of MIMO antenna using novel EBG and hair-pin shaped DGS at 5G millimeter wave band. IEEE Access. 2021 Dec 6; 9: 162820–34.
8. Goswami C, Roy B, Bhattacharya PP, Ray S, Ghosh S, Ghosh D, Saha D, Jana T, Chatterjee S. Complementary split rings resonator based circular microstrip antenna for wireless applications. In 2019 IEEE International Electromagnetics and Antenna Conference (IEMANTENNA). 2019 Oct 17; 065–067.
9. Chen ZN, Liu D, Nakano H, Qing X, Zwick T. Handbook of antenna technologies. Singapore: Springer Publishing Company, Incorporated; 2016 Sep 17.
10. Chen Z, Tang MC, Wang Y, Li M, Li D. Mutual coupling reduction using planar parasitic resonators for wideband, dual-polarized, high-density patch arrays. In 2019 IEEE MTT-S International Wireless Symposium (IWS). 2019 May 19; 1–3.
11. Iqbal A, Saraereh OA, Ahmad AW, Bashir S. Mutual coupling reduction using F-shaped stubs in UWB-MIMO antenna. IEEE Access. 2017 Dec 19; 6: 2755–9.
12. Chandel R, Gautam AK, Rambabu K. Tapered fed compact UWB MIMO-diversity antenna with dual band-notched characteristics. IEEE Trans Antennas Propag. 2018 Feb 7; 66(4): 1677–84.
13. Karaboikis, Soras, Tsachtsiris, Makios. Compact dual-printed inverted-F antenna diversity systems for portable wireless devices. IEEE Antennas Wirel Propag Lett. 2004; 3: 9–14.
14. Li Z, Yin C, Zhu X. Compact UWB MIMO Vivaldi antenna with dual band-notched characteristics. IEEE Access. 2019 Mar 20; 7: 38696–701.
15. Suganya E, Prabhu T, Palanisamy S, Malik PK, Bilandi N, Gehlot A. An isolation improvement for closely spaced MIMO antenna using λ/4 distance for WLAN applications. Int J Antennas Propag. 2023; 2023(1): 4839134.
16. Nasri NE, Ghzaoui ME, Fattah M, Jamil MO, Qjidaa H. A new four ports multiple input multiple output antenna with high isolation for 5G mobile application. In International Conference on Digital Technologies and Applications. Cham: Springer Nature Switzerland; 2023 Jan 27; 264–271.
17. John DM, Vincent S, Nayak K, Supreetha BS, Ali T, Kumar P, Pathan S. A compact flexible four-element dual-band antenna using a unique defective ground decoupling structure for Sub-6 GHz wearable applications. Results Eng. 2024 Mar 1; 21: 101900.
18. Cao TN, Nguyen MT, Phan HL, Nguyen DD, Vu DL, Nguyen TQ, Kim JM. Millimeter-Wave Broadband MIMO Antenna Using Metasurfaces for 5G Cellular Networks. Int J RF Microw Comput-Aided Eng. 2023; 2023(1): 9938824.
19. Kiouach F, El Ghzaoui M, Das S, Islam T, Madhav BT. A compact wideband printed 4× 4 MIMO antenna with high gain and circular polarization characteristics for mm-wave 5G NR n260 applications. Wirel Pers Commun. 2023 Dec; 133(3): 1857–86.
20. Bellona S, Gowthami G, Kumar O, Ali T. A dual side-plate millimeter-wave antenna for 5g applications. Telecommun Radio Eng. 2020; 79(9): 743–751.
21. Thomas SJ, Fatima M. Bandwidth improvement of microstrip patch antenna using partial ground plane. Int J Eng Res. 2015 May; 4(5): 87–91.
22. Ndujiuba CU, Ilesanmi OA, Agboje OE. Bandwidth enhancement of an inset-fed rectangular patch antenna using partial ground with edge-cut method. Int J Electromagn Appl. 2017 Jun; 7(1): 9–16.
23. Votis C, Tatsis G, Kostarakis P. Envelope correlation parameter measurements in a MIMO antenna array configuration. International Journal of Communications, Network and System Sciences (IJCNS). 2010 Apr 1; 3(4): 350–354.
24. Raj T, Mishra R, Kumar P, Kapoor A. Advances in MIMO antenna design for 5G: A comprehensive review. Sensors. 2023 Jul 12; 23(14): 6329.

25. Yousef AS, Abdelraheem A, Abdalla MA, Mahran A. UWB MIMO antenna with hybrid pattern and polarization diversity. J Eng Sci Military Technol. 2021 Sep 1; 5(2): 77–90.
26. Urimubenshi F, Konditi DB, de Dieu Iyakaremye J, Mpele PM, Munyaneza A. A novel approach for low mutual coupling and ultra-compact Two Port MIMO antenna development for UWB wireless application. Heliyon. 2022 Mar 1; 8(3): e09057.
27. Tian R, Lau BK, Ying Z. Multiplexing efficiency of MIMO antennas. IEEE Antennas Wirel Propag Lett. 2011 Mar 10; 10: 183–6.
28. Manteghi M, Rahmat-Samii Y. Broadband characterization of the total active reflection coefficient of multiport antennas. In IEEE antennas and propagation society international symposium. Digest. Held in conjunction with: USNC/CNC/URSI north American radio Sci. Meeting (cat. No. 03CH37450). 2003 Jun 22; 3: 20–23.
29. Chae SH, Oh SK, Park SO. Analysis of mutual coupling, correlations, and TARC in WiBro MIMO array antenna. IEEE Antennas Wirel Propag Lett. 2007 Apr 10; 6: 122–5.
30. Glazunov AA, Molisch AF, Tufvesson F. Mean effective gain of antennas in a wireless channel. IET Microw Antennas Propag. 2009 Mar 1; 3(2): 214–27.

